Development Behavior of Vaporizing Sprays from a High-Pressure Swirl Injector Using Exciplex Fluorescence Method

Dong-Seok Choi, Duck-Jool Kim*
Research Institute of Mechanical Technology, Pusan National University
Soon-Chul Hwang
Graduate school, Department of Mechanical Engineering, Pusan National University

The effects of ambient conditions on vaporizing sprays from a high-pressure swirl injector were investigated by an exciplex fluorescence method. Dopants used were 2% fluorobenzene and 9% DEMA (diethyl-methyl-amine) in 89% solution of hexane by volume. In order to examine the behavior of liquid and vapor phases inside of vaporizing sprays, ambient temperatures and pressures similar to engine atmospheres were set. It was found that the ambient pressure had a significant effect on the axial growth of spray, while ambient temperature had a great influence on the radial growth. The spatial distribution of vapor phase at temperatures above 473K became wider than that of liquid phase after half of injection duration. From the analysis of the area ratio for each phase, the middle part (region II) in the divided region was the region which liquid and vapor phases intersect. For liquid phase, fluorescence-intensity ratio was greatly changed at 1ms after the start of injection. However, the ratio of vapor phase was nearly uniform in each divided region throughout the injection.

Key Words : Gasoline Direct Injection Engine, Exciplex Fluorescence, High-pressure Swirl Injector, Fluorescence Intensity, Spray Tip Penetration, Spray Width

1. Introduction

Gasoline direct-injection (GDI) engines have been developed to overcome the limits of port -fuel injected (PFI) engines and to improve the fuel economy and power density of engines. However, all of the fuel economy can be achieved, while controlling of emissions, such as hydrocarbon, nitric oxide, and even soot, is required (Zhao et al., 1997; Houston and Cathcart, 1998; Wirth et al., 1998; Lee et al., 1998). The spatial distribution of fuel vapor is also an important consideration for determining the location of spark plug. Thus, it is necessary to understand the behavior of liquid and vapor phases inside of vaporizing sprays from high-pressure swirl injectors under various ambient conditions.

The exciplex fluorescence method, which could separately measure the liquid and vapor phases in vaporizing sprays, was introduced by Melton (1983). Ghandhi et al. (1994) used fluorobenzene and DEMA (diethyl-methyl-amine) as dopants in the solution of hexane and quoted that this exciplex system was closely co-evaporated. In the previous study (Choi et al., 1999), the simultaneous visualization of liquid and vapor phases and the quantification of concentration for vapor phase were performed by using the same exciplex system. Han et al. (1997) computed the internal structure of vaporizing pressure-swirl sprays. The computed results indicated that the fuel vapor exhibited a solid-cone distribution in the spray region, while the liquid spray keeps a hollow-cone structure. VanDerWege et al. (1998) showed that the structure of the spray from a pressure-

* Corresponding Author,
E-mail : djkim@hyowon.pusan.ac.kr
TEL : +82-51-510-1386 ; **FAX** : +82-51-510-9598
Research Institute of Mechanical Technology, Pusan National University, San 30, Changjeon-dong Keumjeong-ku, Pusan 609-735, Korea (Manuscript **Received** October 19, 1999 ; **Revised** July 4, 2000)

swirl injector was strongly affected by the fuel component volatility and the local temperatures and pressures. Ipp et al. (1999) experimentally investigated the spray formation for a high-pressure swirl injector. The results showed that the vapor phase followed the liquid phase throughout the injection process. However, the previous experimental studies on the behavior of liquid and vapor phases inside of vaporizing sprays were scarcely performed.

The objective of the present study is to investigate the development behavior of vaporizing sprays from a high-pressure swirl injector through phase separation. The following items were examined in detail: the effect of ambient conditions on the growth of vaporizing sprays, phase effect on the spray shape, temporal changes in the spatial distribution of vapor phase, and the behavior of liquid and vapor phases in the divided regions inside of spray.

2. Experimental

Figure 1 shows the experimental setup used for investigating the high-pressure swirl sprays.

The spray chamber was designed to analyze the behavior and structure of vaporizing sprays under high pressures and high temperatures. The possible maximum ambient temperature and pressure were 600K and 3MPa, respectively. Nitrogen was used as an ambient gas to prevent the quenching of liquid and vapor fluorescence by oxygen. In order to maintain a much more uniform ambient temperature profile within the test section of spray, nitrogen flow passed through the spray chamber at the velocity of less than 0. 1m/s. The spray chamber was purged with nitrogen and then evacuated to remove exciplex-forming dopants from previous measurements. Four different ambient temperatures of 293k, 360K, 473K, and 573K and three different ambient pressures of 0. 1MPa, 0.6MPa, and 1.1MPa were set.

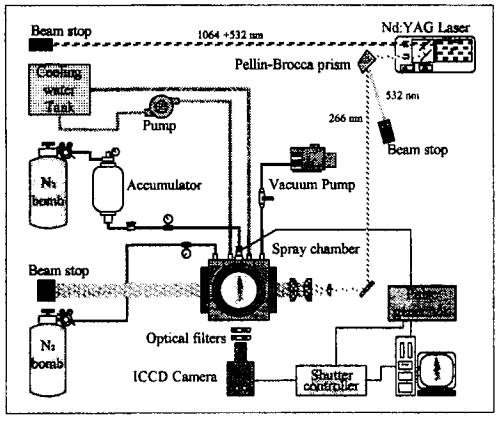

Fig. 1 Schematic diagram of experimental setup

The high fuel pressure required for direct fuel injection were generated using a compressed nitrogen cylinder and a hydraulic accumulator in order to avoid pressure fluctuations in the fuel line. The injector used was a high-pressure swirl injector with a cone angle of 26°. Injection pressure was 5. 1MPa as line pressure and injection duration was 2.2ms.

An intensified-CCD camera was used to capture the images. The camera system consisted of a personal computer with an image grabber, a shutter controller, and a pulse generator. The CCD array had 640 rows and 480 columns of pixels.

The exciplex system of fluorobenzene and DEMA in a non-fluorescing base fuel of hexane was employed. The boiling points for fluorobenzene, DEMA, and hexane were 358K, 338K, and 342K, respectively and the solution composition was 2%/9%/89% by volume respectively. The fourth harmonic of the Nd:YAG (266nm, approximately 50mJ/pulse) was used to excite dopants from the fuel sprays. The laser beam was formed to a thin light sheet of 60mm height and less than 400m thickness. The filters used were 300 ± 25nm (vapor phase) and 400 ± 25nm (liquid phase). An additional sharp cut filter (passing wavelength $>$ 280nm) was used to eliminate the light at 266nm.

3. Results and Discussion

3.1 Characteristics of dopants and filters

Figure 2 shows fluorescence spectra of liquid and vapor phases and transmission spectra of the filters used. The fluorescence spectra of fluorobenzene and exciplex had a peak at the wavelength of 290nm and 380nm, respectively. Vapor-phase

signal was collected through a filter centered at 295nm with a 25nm FWHM (full width half maximum), and its transmittance was 25%. Liquid-phase signal was collected through a filter centered at 400nm with 25nm FWHM, and its transmittance was 50%.

3.2 Axial profiles of liquid and vapor signal

Figure 3 shows the profiles of liquid and vapor phases signals along the spray axis as a function of time after the start of injection. Ambient conditions are at the temperature of 473K and the pressure of 0.6 MPa (approximately 60 degree BTDC).

Y/Y_{max} in Fig. 3 (a) and (b) represents the ratio of spray tip penetration at each time to maximum one throughout the injection. I/I_{max} represents the ratio of fluorescence intensity at each time to maximum one throughout the injection. For the case of liquid phase, fluorescence -intensity ratio was decreased with time after the start of injection. High intensity ratio was initially observed near the injector tip due to dense fuels. Especially, at the time of 1ms after the injection start, intensity ratio was greater at the leading edge of spray because of the leading mass. Moreover, fluorescence-intensity ratio of liquid phase was diminished with time. On the other hand, that of vapor phase had high value downstream.

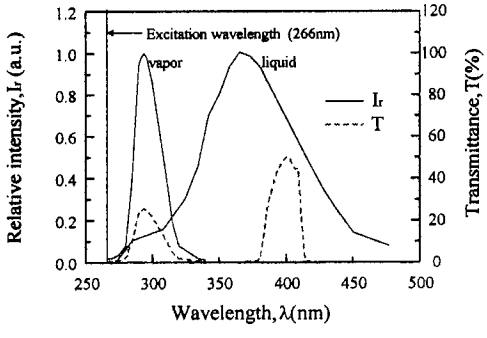

Fig. 2 Fluorescence spectra of both phases and transmission spectra of the filters used

3.3 Spray penetration and width

Figure 4 shows the spray tip penetrations for liquid and vapor phases at different ambient temperatures and pressures. The spray tip penetration after 60mm from the injector tip could not be measured due to the restriction of the field of view. The spray tip penetrations of both phases were increased with time after the start of injection. The higher ambient pressure became, the smaller those of both phases became. With an increase in ambient temperature under constant ambient pressure, those of both phases were decreased. This result indicated that the ambient pressure had a much more effect on spray tip penetration than the ambient temperature.

Figure 5 shows the spray widths for liquid and vapor phases at different ambient temperatures and pressures. The spray width was defined as the maximum radial distance from the spray axis in the incident direction of laser-light sheet. The spray widths of both phases were increased with

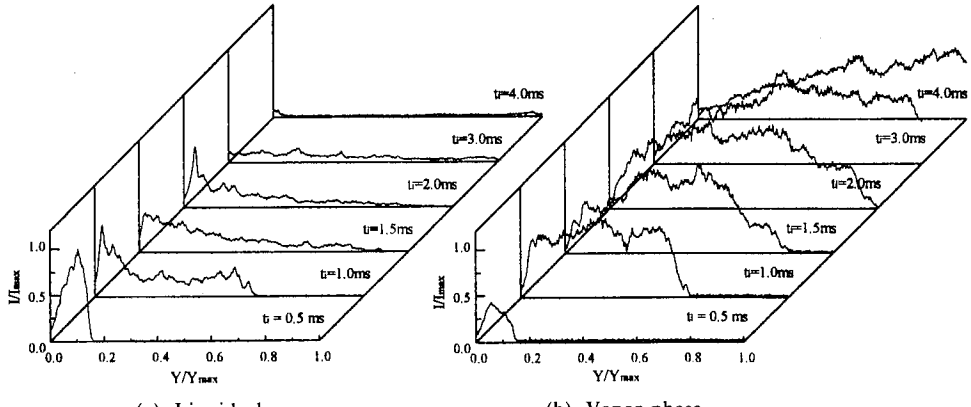

(a) Liquid phase (b) Vapor phase

Fig. 3 Intensity profiles for liquid and vapor phases along the spray axis line

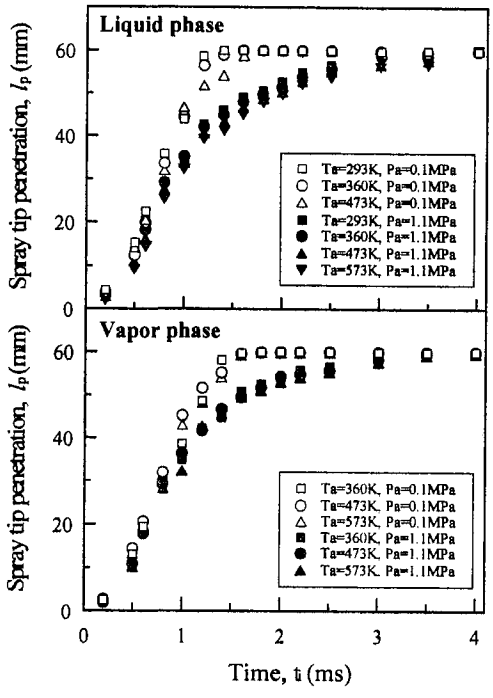

Fig. 4 Temporal changes in spray tip penetration for liquid and vapor phases

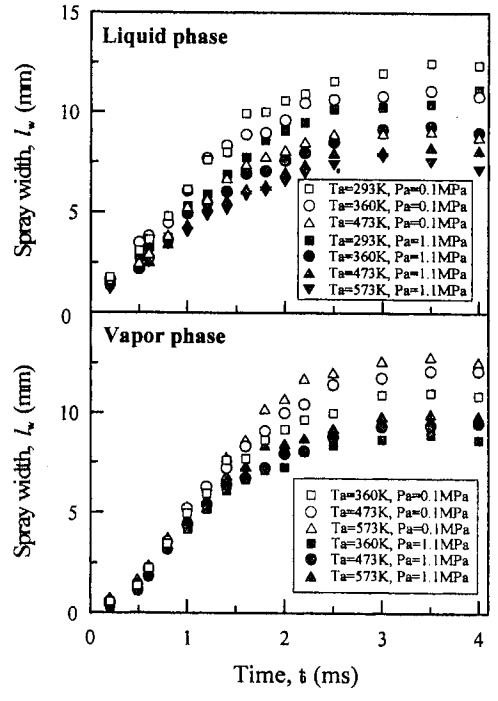

Fig. 5 Temporal changes in spray width for liquid and vapor phases

time after the start of injection. With an increase in ambient temperature at the constant ambient pressure, the spray width for liquid phase was greatly decreased while that for vapor phase was significantly increased. However, the spray widths for both phases were decreased when the ambient pressure was increased under constant temperature condition. This indicated that the ambient temperature had a more significant effect on the spray width than the ambient pressure. After the end of injection (e. g., 3ms), the spray width was slightly decreased due to the rapid spreading of both phases outside the field of view.

3.4 Spray formation under different ambient conditions

Figure 6 shows the development behavior of a vaporizing spray under different ambient conditions with time after the start of injection. The ambient conditions were 0.1MPa and 360K in Fig. 6 (a), 0.6MPa and 473K in Fig. 6 (b), and 1.1MPa and 573K in Fig. 6 (c). These conditions were close to those in an engine when the injection started at 180, 60, and 30 degrees BTDC, respectively. Five spray images for liquid and vapor phases at each time were averaged. The images of left and right sides at each time represent liquid and vapor phases, respectively. In Fig. 6 (a), near the boiling point of hexane, the liquid phase had a strong signal near the injector tip and was developed into the structure of hollow cone with time after the start of injection. However, as the ambient temperature and pressure was increased, the spray angle was decreased and the shape of the spray became compact. Vapor phase distributed inside the sprays and had a strong signal near the spray axis at the elevated ambient temperatures and pressures. In addition, vapor one kept the shape of a solid-cone regardless of the ambient pressure. With an increase in the ambient temperature and pressure, a decrease in spray tip penetration appeared apparently. As described in Han's computational results (1997), the fuel vapor exhibiting a solid-cone distribution soon after the start of injection was experimentally observed. This could be resulting from the breakup processes of the initial spray that consists of a series of collision with fuels injected by

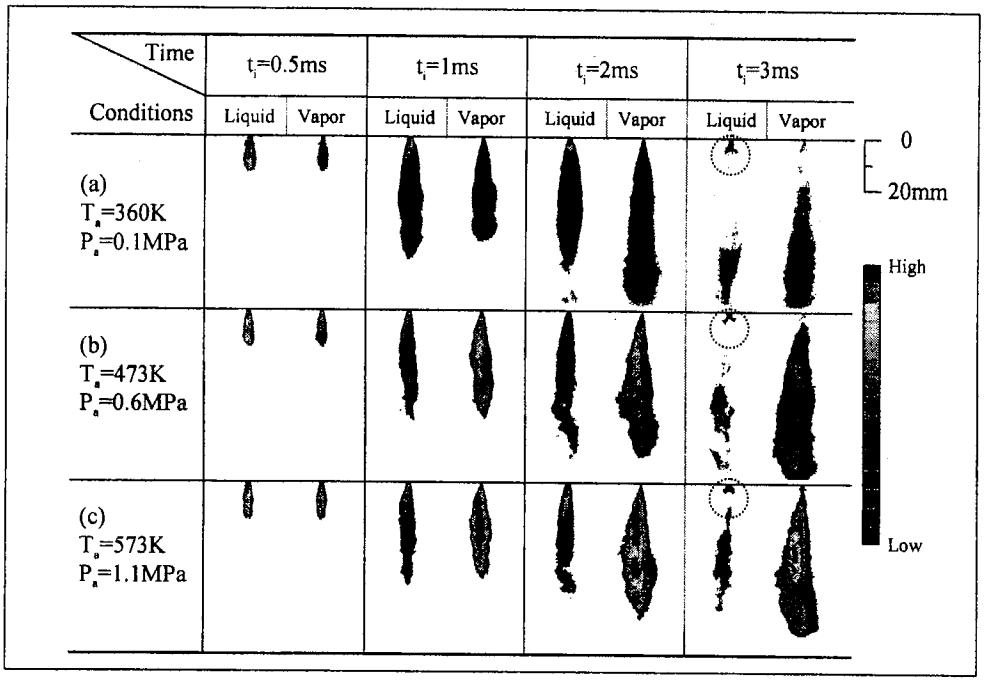

Fig. 6 Evolution of liquid and vapor phases in a vaporizing spray under different ambient conditions

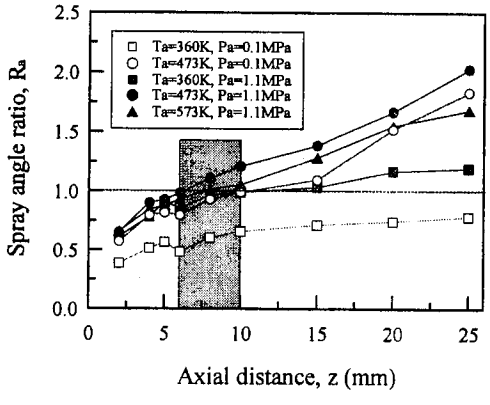

Fig. 7 Changes in spray angle near injector tip

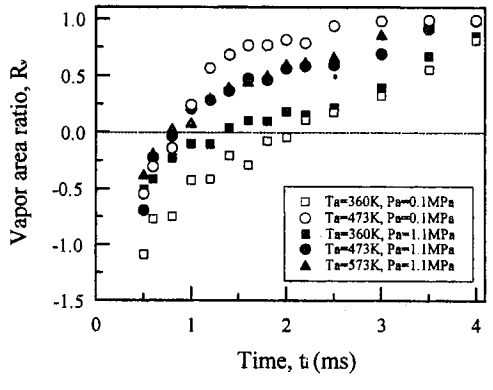

Fig. 8 Temporal changes in the spatial distribution of vapor phase

transient injection pressures (Choi et al., 1998). At the time of 3ms, fuel injected due to the needle bounce, which was marked as dotted circles in Fig. 6, was observed and most fuel vapor was distributed downstream.

Figure 7 shows the spray-angle ratio (R_a) near injector tip. The ratio was defined as the ratio of the cone angle of vapor phase to that of liquid phase. Specific axial positions which R_a had a value of unity were existed. With an increase in ambient temperature, this position approached near the injector tip because of active vaporization of the spray. The axial position ranged from 6mm to 10mm from injector tip except the ambient condition of 360K and 0.1MPa. In the upside of this position, liquid phase determines a spray shape, while vapor phase dominates a spray shape in the downside of this position.

3.5 Spatial distribution and intensity ratio of both phases

Figure 8 shows the temporal change in the

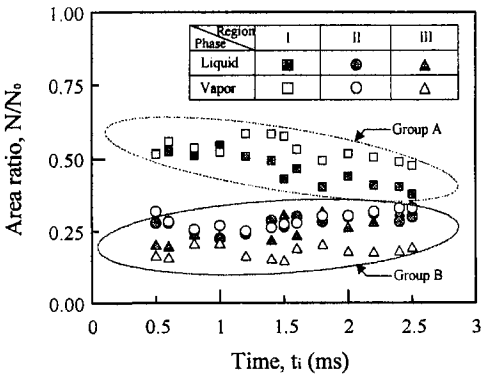

Fig. 9 Temporal changes in spatial distribution for both phases in the divided regions

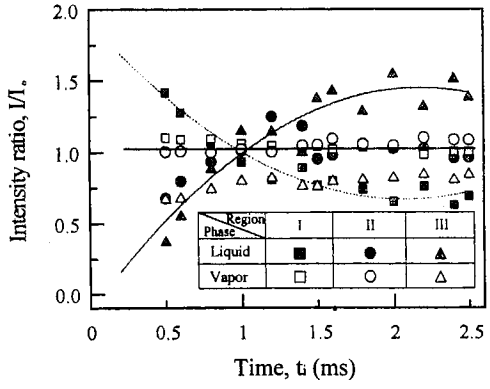

Fig. 10 Temporal changes in intensity for both phases in the divided regions

spatial distribution of vapor phase under different ambient conditions. In order to investigate the spatial distributions of vapor phase only, the vapor-area ratio (R_v) was defined as follows:

$$R_v = (N_v - N_l)/N_v$$

where N_v and N_l are the number of pixels occupied by vapor and liquid phases in the images captured, respectively. If the vapor-area ratio has a positive value, the spatial distribution of vapor phase is wider than that of liquid phase. On the other hand, if it has a negative value, liquid phase is distributed wider than vapor phase. A value of unity means that liquid spray is perfectly vaporized into fuel vapor, while a value of zero means that both phases have the same spatial distribution.

At the ambient pressure of 0.1MPa, the time that Rv approaches zero was rapidly faster as ambient temperature was elevated. At the ambient pressure of 1.1MPa the time mentioned above was also sooner as the ambient temperature was elevated. However, the change in a value of R_v was not nearly at the temperature above 473K for the temperature range examined, and the extent of changes in a value of R_v for each ambient temperature was smaller than case of the ambient pressure of 0. 1MPa. In addition, the vapor-area ratio became zero at about 1ms (approximately half of injection duration) after the start of injection at temperatures above 473K. From these results, the spatial distribution of vapor phase is affected by ambient temperature more in low ambient pressure than in high ambient pressure.

Figures. 9 and 10 show the development behavior of liquid and vapor phases inside a vaporizing spray under the ambient condition of 573K and 1. 1MPa. Three regions were divided by trisecting a spray half-angle: near the spray axis (region I), middle of the spray (region II), and periphery of the spray (region III). The spray half-angle was defined as the interior angle between the spray-axis line and a straight line drawn from the injector tip to cut the spray contour at 1/3 of spray tip penetration at each time after the start of injection. The area ratio was defined as the ratio of the number (N) of pixels occupied by each phase in each region to that (N_0) for each one in the left half region of spray. Also, fluorescence-intensity ratio was defined as the ratio of fluorescence intensity (I) for each phase in each region to that (I_0) for each phase in the left half region of spray. Although not shown here, the ratios under other ambient conditions also showed similar results to those in Figs. 9 and 10.

Figure 9 shows the change in the spatial distribution for liquid and vapor phases in three regions with time after the start of injection. Area ratios in the region I and in other regions were classified group A and B, respectively. For region I, the area ratio of liquid phase was decreased because droplets move outside of spray due to the typical characteristics of swirl sprays. On the other hand, the ratio of vapor phase was nearly

maintained constant. For region II, the ratio of liquid phase was slightly increased due to the droplets moved from the region I. The ratio of vapor phase was also increased due to vaporization of small droplets entrained with ambient gas. Therefore, it is presumed that this region is the one which liquid and vapor phases intersect. For region III, the ratio of liquid phase was increased due to large droplets outside of spray. However, the ratio of vapor phase was nearly constant. This was caused by poor vaporization of large droplets distributed in this region.

Figure 10 shows the change in the fluorescence -intensity ratio for liquid and vapor phases. For liquid phase, the ratio in the region I was decreased with time after the start of injection, while the ratio in the region III was increased. For vapor phase, the ratio was appeared nearly the same in the region I and II, and was somewhat smaller in the region III than in the others. The ratio was, nevertheless, nearly constant in each region with time after the start of injection. Thus, the region II implies the region which liquid and vapor phases intersect, as described in Fig. 9. It is presumed that the time of 1ms when the spatial distribution of liquid and vapor phases was the same, as mentioned in Fig. 8, is a characteristic time.

4. Conclusions

This research examined the development behavior of high-pressure swirl sprays at different ambient temperatures and pressures. In order to separate liquid and vapor phases from vaporizing sprays, the exciplex fluorescence method was used. The main results were summarized as follows:

(1) The ambient pressure had a significant effect on the axial growth of spray, while the ambient temperature had a great influence on the radial growth.

(2) Specific axial positions which spray-angle ratio had a value of unity were existed. Liquid phase determined a spray shape in the upside of this position, while vapor phase dominated a spray shape in the downside of this position.

(3) After about 1ms, half of injection duration, the spatial distribution of vapor phase at temperatures above 473K became wider than that of liquid phase.

(4) From area ratio and fluorescence-intensity ratio for each phase, the middle part (region II) in the divided region was the region which liquid and vapor phases interseced.

References

Choi, D. S., Kim, D. J., and Ko, C. K., 1998, "Transient Breakup Phenomena of Initial Spray from High-Pressure Swirl Injector," *Trans. of KSME (B)*, Vol. 22, No. 8, pp. 1132~1140, (in Korean).

Choi, D. S., Park, H. H. and Kim, D. J., 1999, "Measurement of Distribution and Concentration of Vapor/Liquid Phases in Gasoline Direct Injection Spray Using Exciplex Fluorescence Method," *Trans. of KSME (B)*, Vol. 23, No. 4, pp. 531~539, (in Korean).

Ghandhi, J. B., Felton, P. G., Gajdeczko, B. F. and Brocco, F. V., 1994, "Investigation of the Fuel Distribution in a Two-Stroke Engine with and Air-Assisted Injector," *SAE paper*, No. 940394.

Han, Z. and Reitz, R. D., 1997, "Internal Structure of Vaporizing Pressure-Swirl Fuel Sprays," *Proc. ICLASS-97*, pp. 474~481.

Houston, R. and Cathcart, G., 1998, "Combustion and Emissions Characteristics of Orbital's Combustion Process Applied to Multi-Cylinder Automotive Direct Injected 4-Stroke Engines," *SAE paper*, No. 980153.

Ipp, W., Wagner, V., Krmer, H., Wensing, M., Leipertz, A., Arndt, S. and Jain, A. K., 1999, "Spray Formation of High Pressure Swirl Gasoline Injectors Investigated by Two-Dimensional Mie and LIEF Techniques," *SAE paper*, No. 1999-01-0498.

Lee, N. H., Park, J. H. and Choi, K. H., 1998, "A Study on Fuel Spray of Spark-Ignited Direct Injection Engine Using Laser Image Technology," *KSME International Journal*, Vol. 13, No. 3, pp. 286~293.

Melton, L. A., 1983, "Spectrally Separated

Fluorescence Emissions for Diesel Fuel Droplets and Vapor," *Applied Optics*, Vol. 22, No. 14, pp. 2224~2226.

VanDerWege, B. A. and Hochgreb, S., 1998, "The Effect of Fuel Volatility on Sprays from High-Pressure Swirl Injectors," *Int. Symp. COMODIA 98*, pp. 505~510.

Wirth, M., Piock, W. F., Fraidl, G. K., Schoeggl, P. and Winklhofer, E., 1998, "Gasoline DI Engines: The Complete System Approach by Interaction of Advanced Development Tools," *SAE paper*, No. 980492.

Zhao, F. -Q., Lai, M. -C. and Harrington, D. I., 1997, "A Review of Mixture Preparation and Combustion Control Strategies for Spark-Ignited Direct-Injection Gasoline Engine," *SAE paper*, No. 970627.